Volatile Organic Compound Specialists in the Phycosphere

Authors: Vaishnavi G. Padaki[1], Xavier Mayali[2], Peter K. Weber[2], Stephen J. Giovannoni[1], Kaylene Abraham[1], Kerry Jacobs[1], Lindsay Collart[1], Kimberly H. Halsey[1*]

Author Affiliations:

[1] Department of Microbiology, Oregon State University

[2] Lawrence Livermore National Laboratory, Livermore, CA 94550 USA

[*]corresponding author

Abstract:

Labile dissolved organic carbon (LDOC) in the oceans accounts for ~ ¼ of global photosynthesis and turns over with a half-life of about one day, fueling one of the largest engines of microbial heterotrophic production on the planet. Volatile organic compounds (VOCs) are poorly constrained components of LDOC. We detected 78 VOCs totaling 18.5 μM in cultures of the model diatom *Phaeodactylum tricornutum*, including hydrocarbons usually found in petroleum. In five individual cocultures with bacteria adapted to grow with this diatom, 1 to 66 VOCs were depleted. Two of the most active VOC consumers, *Marinobacter* and *Roseibium,* had more VOC oxidation genes, and attached to the diatom, suggesting VOC specialism. Diatom photosynthesis increased by up to 29% in the presence of VOC consumers, indicating that VOC consumption by heterotrophic bacteria in the phycosphere – a region of rapid organic carbon oxidation that surrounds phytoplankton cells – could impact global rates of primary production.

Main:

The phycosphere, the layer of water immediately surrounding an algal cell, is the site of complex interactions between phytoplankton and bacterioplankton, which influence carbon and nutrient cycling in marine ecosystems [1–3]. Microbial activities in the phycosphere are distinct from processes occurring in bulk water, a result of bacterial taxa with specialized adaptations populating the region of concentrated chemicals surrounding phytoplankton [4,5]. Direct chemical transfer from phytoplankton to bacterioplankton is enhanced by their occupation of the narrow zone of the phycosphere, which allows access to metabolites before they diffuse into the bulk seawater [2,6]. The ecology of the phycosphere is similar to its terrestrial analog, the rhizosphere;

29 phylogenetically related bacterial taxa are found across both systems [7], chemotaxis plays a
30 central role in accessing the narrow zone of high chemical concentration [8,9], and the chemicals
31 transferred from the primary and secondary producers are functionally similar [2]. For example,
32 primary metabolites, such as sugars, amino acids, and vitamins, as well as metabolite precursors,
33 such as organosulfur compounds (dimethylsulfide (DMS) and dimethylsulfoniopropionate) [10,11],
34 are used as bacterial growth substrates in the phycosphere and rhizosphere [12,13].

35 Volatile organic compounds (VOCs) are an important subset of the labile dissolved
36 organic compounds (LDOC) produced by phytoplankton, but VOCs are often overlooked in
37 metabolomic studies because most are not captured by common methods of analysis such as
38 solid phase extraction and liquid chromatography. VOCs are relatively low in molecular weight,
39 hydrophobic, and can diffuse across cell membranes. Some VOCs, such as isoprene and DMS,
40 are produced by phytoplankton in response to stress [14–16], while others (e.g., acetaldehyde and
41 methyl iodide) are intermediate chemicals in metabolic pathways [17,18]. Due to their diffusive
42 properties, these VOCs may escape biochemical transformation and cross the algal cell
43 membrane into the phycosphere. Other VOCs, including aromatic benzenoids such as benzene,
44 toluene, and ethylbenzene/xylene (collectively known as BTEX), are produced by phytoplankton
45 via the shikimate and non-mevalonate pathways [19,20], but the specific reactions involved in
46 BTEX formation are not known.

47 Research on VOC transfer between algae and bacteria is sparse but suggests VOCs
48 released by algae can be growth substrates for marine bacteria. A wide range of VOCs were
49 detected during the growth of the diatom, *Thalassiosira pseudonana*, and a subset of those
50 supported the growth of *Pelagibacter ubique* HTCC1062, a member of ubiquitous SAR11
51 bacterioplankton [18,21]. These publications suggested that VOCs were "public goods" released by

52 the diatom constitutively and available to any organism able to metabolize them. HTCC1062
53 metabolizes isoprene, acetone, acetaldehyde, DMS, and cyclohexanol, which are some of the
54 most well-studied VOCs for their roles in sea-air exchange and atmospheric chemistry [18]. BTEX
55 are produced by some algae [19], and are growth substrates for a wide variety of bacteria isolated
56 from oilfields [22,23], soils [24], groundwater [25], and wastewater [26]. Less is known about BTEX
57 consumption by marine bacteria, which is likely an important sink that limits BTEX emissions
58 into the atmosphere [27]. Genetic mechanisms underlying bacterial metabolism of some VOCs
59 (e.g., methanol, DMS, acetone, acetaldehyde) have been elucidated [18,28,29]. The widespread
60 expression of some of the genes involved, such as acetone/cyclohexanone monooxygenase,
61 suggests marine bacteria have an important role in mediating VOC sea-air emissions [18].
62 However, the full diversity of VOCs used by bacteria in the oceans is unknown.

63 The bacterial community in the phycosphere of marine microalgae may be uniquely
64 adapted to VOC metabolism, as is the case for methylotrophs in the phyllosphere [30]. The
65 phycosphere of a modest-sized (~20 μm) diatom extends about 50 – 2000 μm away from the cell
66 [2]. In this region, chemicals are modeled to be ≥50% higher than in bulk seawater [2], where VOC
67 concentrations are in the pM to nM range. VOC concentration in the phycosphere is partly
68 controlled by the rate of diffusion from the algal source. The rate of diffusion decreases with
69 increased molecular size and decreased hydrophobicity and likely increases with phytoplankton
70 growth rate and bacterial VOC uptake. Some bacteria occupy the phycosphere through
71 chemotaxis or physical attachment to algal cells [31,32]. Chemotactic bacteria experience transient
72 exposures to a dynamic organic chemical cocktail in the phycosphere [12], where the composition
73 depends on the algal producer [1,33], environment [34,35], and antagonistic and mutualistic
74 interactions [12,36,37], requiring bacterial consumers to efficiently shift physiologies to match

resource availability. Strategies bacteria use to navigate carbon acquisition as they traverse phycosphere boundaries are not known but may depend on pool sizes and the diversity of regulatory behavior systems for the uptake and metabolism of various substrates [38]. Bacteria that can adhere to algae would, in principle, optimize diffusion-mediated VOC uptake by maximizing areal coverage of VOC flux directly from the algal source.

Here, we investigated VOC transfer from the model diatom, *Phaeodactylum tricornutum,* to phycosphere bacteria previously isolated from a large-scale *P. tricornutum* production pond. The bacteria varied in taxonomy, DOC uptake, and attachment to the diatom [12,39,40]. Results show significant VOC transfer from *P. tricornutum* to its phycosphere bacteria, fueling primary and secondary production. Extrapolated to larger scales, our findings support the perspective that phycosphere bacteria are a sink for up to 29% of primary production and play an important role in limiting VOC accumulation in the surface ocean.

Results:

Phaeodactylum tricornutum produced a wide range of VOCs in culture

During exponential growth of *P. tricornutum*, 78 m/z signals were detected by proton transfer reaction mass spectrometry (PTR-MS) at concentrations higher than the media control (Benjamini-Hochberg, Q-value < 0.1, n = 6). VOCs accumulated to a total of 85.1 pM $cell^{-1}$ and represented nine chemical functional groups (Fig. 1). Hydrocarbons represented about 60% of the VOCs produced in the exponential phase (54.2 pM $cell^{-1}$; Supp. table 1). The benzenoid class of aromatic hydrocarbons was most abundantly produced, including BTEX compounds (m/z 79.11, m/z 93.07, and m/z 107.08), respectively [19], and $C_{11}H_{16}^{+}$ (m/z 149.13). Note that in PTR-MS, VOCs are detected at their protonated ion masses. Alcohols were the second most

97 abundantly produced group of VOCs, contributing up to 11% of the total VOC pool (10.20 pM
98 cell^{-1}). Methanol (m/z 33.03) and, likely, ethanol (m/z 47.04) made up the vast majority of the
99 accumulated alcohols (Fig.1, Supp. table 1). Consistent with reports that *P. tricornutum* is a
100 halocarbon producer [41,42], m/z 124.96, corresponding to ethyl bromide, was detected in the
101 exponential phase. The well-studied VOCs acetone (m/z 59.05), acetaldehyde (m/z 45.03), and
102 DMS (m/z 68.07) were also detected in the exponential phase (Fig. 1, Supp. table 1).

103 After *P. tricornutum* entered the stationary growth phase, 58 m/z signals were detected in
104 concentrations higher than the media control (Benjamini-Hochberg, Q-value < 0.1, n = 6) and
105 accumulated to 9.01 pM cell^{-1} (Fig. 1), which was only about 10% of the VOC accumulation
106 during the exponential phase (Fig. 1, Supp. table 1). VOCs detected in both phases of growth
107 were consistently lower in concentration in the stationary phase. Slower VOC production in
108 response to cessation of growth, and loss of VOCs from the vented growth flasks, are the most
109 likely explanations for the concentration differences between growth phases. Hydrocarbons still
110 represented the majority of the VOCs (84%) but were only 7.59 pM cell^{-1}. Sixteen of the 58 m/z
111 signals were unique to the stationary phase, but many of these had unknown identities.

112 The most abundant VOC in both exponential and stationary phases was $C_{11}H_{16}^{+}$ (m/z
113 149.13) in the benzenoid superclass and corresponds to dictyopterene, an algal sesquiterpenoid
114 pheromone. Chemical isomers of dictyopterene include the aromatic hydrocarbons, neopentyl-
115 benzene, 4-tert-butyl-toluene, and 1-ethyl-2-propylbenzene, which have been identified in plant
116 leaves [43]. Forty-two m/z signals, including BTEX, were detected in both exponential and
117 stationary phases (Fig. 1).

118 *VOCs were depleted in P. tricornutum-bacteria cocultures*

119 Five *P. tricornutum*-bacteria cocultures were grown to identify VOCs produced by the
120 diatom that decreased in concentration in the presence of a bacterium, which would suggest
121 those VOCs were consumed by the bacterium. Alternatively, decreased VOC concentrations in a
122 coculture could indicate VOC production was inhibited in the presence of the bacterium. The
123 five *P. tricornutum*-bacteria cocultures (herein "PT-bacteria genus name") each showed distinct
124 VOC depletion patterns during exponential growth when compared to axenic *P. tricornutum*
125 (Fig. 2a, Supp. Fig. 1; PERMANOVA, p-value = 0.03, n = 6). Of the 78 m/z signals produced by
126 *P. tricornutum* in exponential phase, 31 to 59 were significantly depleted in four of the five
127 cocultures (Benjamini-Hochberg, Q-value cut-off ≤ 0.1, n = 6) (Fig. 2a). VOCs were most
128 strongly depleted in PT-*Marinobacter* (7.09 pM $cell^{-1}$), followed by PT-*Stappia* (6.51 pM $cell^{-1}$),
129 PT-*Roseibium* (5.52 pM $cell^{-1}$) and PT-*Rhodophyticola* (4.54 pM $cell^{-1}$) (Fig. 2a, Fig. 4, Supp.
130 table 1). About half the number of m/z signals were depleted in the PT-*Roseibium* compared to
131 PT-*Marinobacter*. *Marinobacter* and *Roseibium* were observed to be attached to *P. tricornutum*
132 (Fig. 3) [39], thus the cell-normalized VOC depletion data in PT-*Marinobacter* and PT-*Roseibium*
133 are based on estimates of bacteria cell densities using flow cytometry for the free-living and
134 scanning electron microscopy for the attached bacteria (see Methods). In PT-*Yoonia*, only one
135 m/z signal, 45.03, corresponding to acetaldehyde, was significantly depleted (0.5 pM $cell^{-1}$ (Fig.
136 2a)). There were 14 m/z signals that did not show significant depletion in any of the five PT-
137 bacteria cocultures. A lack of depletion could mean that the bacteria could not take up or
138 metabolize those VOCs, or those VOCs were maintained at a steady state concentration by equal
139 rates of production and consumption in the coculture. Of those, 8 m/z signals belonged to the
140 nitrogen-containing class of VOCs (Supp. table 6). Furthermore, neither methanol nor acetone
141 were depleted in any of the five cocultures.

142 Hydrocarbons were the most highly depleted group of VOCs in all PT-bacteria cocultures
143 except PT-*Yoonia*. Depending on the bacterium present, 11-19 of the depleted m/z signals were
144 classified as hydrocarbons and made up to 70% of the total VOC pool depleted in the cocultures.
145 PT-*Marinobacter* depleted the most hydrocarbons (5.95 pM $cell^{-1}$), followed by PT-*Stappia*
146 (5.44 pM $cell^{-1}$), PT-*Roseibium* (4.48 pM $cell^{-1}$) and PT-*Rhodophyticola* (3.94 pM $cell^{-1}$) (Fig.
147 2a). Monoaromatic hydrocarbons, including BTEX, $C_{11}H_{16}^{+}$, and phenylacetylene (m/z 103.05),
148 were the most strongly depleted hydrocarbons in the PT-bacteria cocultures (Fig. 2a).

149 In stationary growth phase, the range of depleted VOCs in the PT-bacteria cocultures was
150 lower, from 0.64-4.97 pM $cell^{-1}$ (average 2.96 ± 0.66 pM $cell^{-1}$). The depletion patterns between
151 PT-bacteria cocultures in stationary phase were not distinct from one another (Fig. 2b,
152 PERMANOVA p-value = 0.22, n = 6). In total, 24 to 55 m/z signals were depleted in the PT-
153 bacteria cocultures (Benjamini-Hochberg, Q-value < 0.1, n = 6). The number of m/z signals
154 depleted in PT-*Yoonia* expanded from 1 in the exponential phase to 24 in the stationary phase,
155 but the amounts of the individual VOCs depleted were low (Fig. 2b, Supp. Table 2 and 3). In
156 stationary phase, 9-16 m/z signals depleted in PT-bacteria cocultures were classified as
157 hydrocarbons, and these VOCs were the majority of the depleted VOC pools (80-92%). VOCs
158 classified as carboxylic acids were the second-most depleted group, followed by ketones (Fig. 2a
159 and b). Except for hydrocarbons, the magnitude of VOC depletion in PT-bacteria cocultures did
160 not mirror VOC abundances in axenic *P. tricornutum* in either growth phase (Fig. 1, Supp. tables
161 1, 2, and 3).

162 *VOC transfer to bacteria comprised up to 30% of primary production*

163 *P. tricornutum* growth rates, chlorophyll content, and photosynthetic efficiencies were
164 unaffected by the presence of any of the bacterial species in the PT-bacteria cocultures (Supp.
165 Table 4). To assess the impact of bacterial VOC uptake on *P. tricornutum* primary production,
166 short-term $^{14}CO_2$-uptake rates, approximating gross carbon production (GCP) were measured.
167 GCP in PT-bacterial co-cultures were higher in PT-*Marinobacter,* PT-*Stappia,* and PT-
168 *Rhodophyticola* than in axenic *P. tricornutum* (Fig. 4). A hydrocarbon trap that stripped VOCs
169 from the axenic *P. tricornutum* culture, simulating a highly efficient bacterial VOC sink, caused
170 GCP to increase 24.9% compared to axenic *P. tricornutum* with no trap (Fig. 4; $p = 0.025$, $n =$
171 6). GCP in PT-*Marinobacter,* PT-*Rhodophyticola,* and PT-*Stappia* were 20.1% to 29.3% higher
172 than in axenic *P. tricornutum,* similar to the hydrocarbon trap-control, and corresponding to 0.27
173 to 0.41 nmol C $cell^{-1}$ h^{-1} transferred to the bacteria in the form of VOCs (p-values < 0.02, t-tests,
174 n=3) (Fig. 4). Consistent with the minimal amount of VOC depleted in PT-*Yoonia* there was no
175 significant difference in CO_2-uptake rates between PT-*Yoonia* and axenic *P. tricornutum* (p-
176 values 0.23, t-test, n=3). Interestingly, GCP was not stimulated in PT-*Roseibium* until *Roseibium*
177 entered the second exponential growth phase in its diauxic growth pattern (Fig. 2; note lag
178 between days 2 and 4). This result suggests that *Roseibium* shifted carbon uptake from primarily
179 LDOC early in culture growth to primarily VOCs later in culture growth.

180 *VOC depletion correlates with genome content for hydrocarbon metabolism*

181 Of the five bacteria tested*, Marinobacter* and *Roseibium* genomes harbor the greatest
182 range of hydrocarbon metabolism genes. For example, genes that initiate hydrocarbon oxidation
183 were identified in *Marinobacter* and *Roseibium,* including *rhdA,* encoding ring hydroxylating
184 dehydrogenase, *almA*, encoding flavin-binding monooxygenase involved in long-chain alkane
185 degradation, and *alkB,* encoding alkane monooxygenase. *rhdA* is in a superclass of nonheme iron

186 enzymes that convert aromatic hydrocarbons to dihydrodiols in the presence of dioxygen and
187 NADH [44]. The broad substrate range for *rhdA* includes benzene, and the benzene-alkyl
188 substituted hydrocarbons toluene, ethylbenzene, and xylene, consistent with BTEX depletion
189 profiles in *Marinobacter* and *Roseibium*. Benzene dioxygenases are a subclass of *rhdA* that
190 oxidize benzene and toluene to their corresponding dihydrodiols. We manually curated the *rhdA*
191 hits for *bnzA*, encoding the α-subunit of the benzene 1,2 dioxygenase hydroxylase based on the
192 conservation of the active site motif Cys-X_1-His-15-to-17 aa-Cys-X_2-His (where X is any amino
193 acid) [45]. *bnzA* was identified in *Marinobacter*, *Rhodophyticola*, and *Roseibium* (Fig. 2d).
194 *Marinobacter* also encodes *bnzB,* the β-subunit of benzene 1,2 dioxygenase hydroxylase (Fig.
195 2d). The presence of both *bnzA* and *bnzB* subunits increases hydroxylation activity compared to
196 the activity of either of the subunits alone [46]. Genes facilitating hydrocarbon oxidation in *Stappia*
197 were not identified. Acetone/cyclohexanone monooxygenase (*acmA*) was identified in
198 *Marinobacter, Roseibium, and Stappia*. The broad substrate range of *acmA* likely includes cyclic
199 ketones, such as valerophenone (m/z 163.11) and E-jasmone (m/z 165.13), corresponding to m/z
200 signals that were depleted in the PT-*Marinobacter*, PT-*Roseibium*, and PT-*Stappia*. All five
201 bacteria encode one or two copies of aldehyde dehydrogenase (*aor*), consistent with
202 acetaldehyde (m/z 45.03) depletion in all five cocultures (Fig. 2).

203 *Marinobacter* and *Rhodophyticola exhibit distinct benzene metabolism*

204 We selected benzene as a representative hydrocarbon to directly test incorporation into
205 biomass by *Marinobacter* and *Rhodophyticola*. These bacteria differed in the amounts of
206 benzene depleted in the PT-bacteria cocultures, in their genetic capacities for hydrocarbon
207 metabolism and chemotaxis, in their attachment physiologies (Fig. 2, 3, 5) [39], and could be
208 grown without *P. tricornutum* in media prepared from filtrate collected from *P. tricornutum* in

209 exponential growth ('PTspent'; see methods). *Marinobacter* and *Rhodophyticola* grew to higher
210 abundances in PT spent medium with added benzene vs. no added benzene (Fig. 5).

211 Benzene uptake and subsequent incorporation into biomass by *Marinobacter* and
212 *Rhodophyticola* were quantified using nanoSIMS. We incubated each bacterium with and
213 without ^{13}C benzene (60 µM in *Marinobacter* cultures, 36 µM in *Rhodophyticola* cultures) and
214 ^{15}N leucine (50 nM) in f/2+Si artificial seawater medium (ASW), PT spent medium, and in
215 coculture with *P. tricornutum*. *Marinobacter* increased its growth in ASW with benzene added
216 as the sole source of carbon (Fig. 5a). Associated C_{net} values of incorporation, measuring the
217 fraction of a cell's C originating from benzene, increased over the incubation period, reaching
218 0.03 to 0.15 (average 0.065) on day 7 (Fig. 5b). *Marinobacter* reached higher cell densities in
219 PTspent with added benzene compared to PTspent with no benzene or ASW with benzene (Fig.
220 5a (p-value <0.05, n = 3). Consistent with benzene-stimulated growth in PTspent, *Marinobacter*
221 C_{net} values in that treatment ranged from 0.02 to 0.17, averaging 0.07 on day 4. *Marinobacter*
222 cell densities were unaffected by benzene addition to PT-*Marinobacter*. Surprisingly,
223 *Marinobacter* did not incorporate ^{13}C benzene in the presence of live *P. tricornutum* cells.
224 *Marinobacter* C_{net} values in the coculture hovered around zero across the 10-day incubation,
225 even in the presence of 60 µM externally-supplied benzene (Fig. 5a,b). Thus, *Marinobacter* did
226 not incorporate measurable quantities of ^{13}C-benzene in the presence of live *P. tricornutum* cells.
227 N_{net} values from leucine in all *Marinobacter* treatments, including the coculture, were low but
228 significant (<0.01, Supp. Fig. 5), confirming bacterial activity.

229 Despite significantly higher *Rhodophyticola* cell densities in PTspent with 36 µM
230 benzene added compared to the no benzene-added control (Fig. 5c). ^{13}C-benzene addition to
231 PTspent resulted in low C_{net} values, and only 2% of the population showed enrichment in ^{13}C

232 benzene on day 6 (Fig. 5d). *Rhodophyticola* may take up and oxidize benzene for energy rather
233 than biomass generation. No significant difference was observed in *Rhodophyticola* cell densities
234 grown in the PT coculture with or without added ^{13}C-benzene. Similar to *Marinobacter*, C_{net}
235 values in *Rhodophyticola* grown in the PT coculture were very low. *Rhodophyticola* showed
236 significant ^{15}N enrichment from leucine in both PTspent and PT-*Rhodophyticola* treatments
237 (Supp. Fig. 5).

238 Discussion

239 Phycospheres are recognized as energy-rich regions of heterotrophic activity where
240 microbes adapted to this niche benefit from proximity to high concentrations of the organic
241 carbon resources produced by phytoplankton cells. VOCs are rapidly diffusing molecules that
242 easily traverse cell membranes and, due to the introduction of new measurement technologies,
243 are increasingly recognized as complex and important products of phytoplankton metabolism.
244 Here, we show that the phycosphere concept applies to VOCs and that they appear to be an
245 important component of photosynthetic carbon transfer to heterotrophic microbial populations in
246 the region immediately surrounding phytoplankton cells. We also show that some phycosphere
247 bacteria have traits that can be interpreted as evidence of VOC specialism, enabling them to
248 access these chemicals whose concentrations are expected to rapidly decrease with distance from
249 their source.

250 VOCs were primarily produced during active *P. tricornutum* growth, when over a quarter
251 of photosynthetically fixed carbon was emitted from *P. tricornutum* as VOCs. Hydrocarbons
252 were 64% of the total VOC produced, with BTEX accounting for 13% of the emitted VOC pool,
253 accumulating to 11.8 μM. BTEX production by phytoplankton has been proposed to be of

254 sufficient magnitude to influence atmospheric chemistry [19], unless bacterial VOC consumption
255 prevents BTEX accumulation in the surface ocean [27]. The VOC concentrations we measured
256 could be underestimated because the cultures were grown in vented flasks. However, in the
257 absence of bacterial sinks, internal VOC concentrations in axenic *P. tricornutum* cells may reach
258 equilibria with the surrounding medium.

259 We measured concentrations of VOCs in diatom-bacteria cocultures relative to diatoms
260 alone to investigate the potential for VOC uptake by bacteria. In the case of benzene, isotopic
261 labeling confirmed that the bacteria were consumers, but for other VOCs, we cannot eliminate
262 the possibility that VOC depletion in coculture was caused by inhibition of VOC production by
263 *P. tricornutum*. *P. tricornutum* photosynthesis (GCP) was stimulated in cocultures where
264 depletion of a wide range of VOCs was also observed. Some marine bacteria are known to
265 metabolize VOCs, including BTEX [21,47], and we show that the bacteria that caused VOC
266 depletion also harbor genes for some of the depleted compounds; for other depleted compounds,
267 genetic loci associated with consumption are unknown and cannot be ruled out.

268 The data we report here indicate a range of VOC specialism (Table 1). Four of the five
269 bacterial strains harbor multiple hydrocarbon oxidation genes that encode enzymes with broad
270 substrate ranges. *Marinobacter* and *Roseibium,* which consumed large amounts of hydrocarbons,
271 had the most genes for hydrocarbon oxidation. *Marinobacter* and *Roseibium* encode few genes
272 for complex polysaccharide metabolism, and in previous research, incorporated low amounts of
273 macromolecular DOC into biomass [39]. In our experiments, *Rhodophyticola* and *Stappia,* which
274 harbor fewer hydrocarbon oxidation genes, depleted smaller amounts of individual hydrocarbons
275 but a wide range. Mayali et al. reported that *Stappia, Rhodophyticola,* and *Yoonia* used complex

276 DOC in the 2023 study, in agreement with their genetic capacities for oligosaccharide, starch,
277 and cellulose degradation. Thus, for this set of traits, among a set of five heterotrophic isolates
278 from *P. tricornutum* ponds, two strains appeared to be VOC specialists: they used more VOCs
279 and less carbohydrate DOM, and as discussed below, they were motile, and attached to *P.*
280 *tricornutum*. Two strains used lesser amounts of VOCs, are active metabolizers of carbohydrate
281 DOM, are not motile, and did not attach; and one strain used carbohydrate DOM, only a single
282 VOC, and attached.

283 We looked for evidence of phycosphere occupation to understand whether, in the strains
284 we studied, it was linked to VOC use. The VOC specialists, *Marinobacter* and *Roseibium,* and
285 one strain that did not use VOCs, *Yoonia*, attached to *P. tricornutum,* but the other strains did
286 not. *Marinobacter* attached to the diatom in a flat orientation, while *Roseibium* attached to *P.*
287 *tricornutum* using polar adhesion (Supp. Fig. 2). It has been reported that chemotaxis and
288 motility are key traits of hydrocarbon-degrading bacteria. Volatile aromatic hydrocarbons,
289 including toluene and benzene derivatives, have been shown in previous work to be effective
290 bacterial chemoattractants, even in the presence of complex organic matter, such as petroleum,
291 crude oil, and diesel [48–50]. *Marinobacter* and *Roseibium* encode canonical chemotaxis *che* genes
292 [39], but chemoattractant compounds have not been identified in these bacteria [8,51] (Table 1).

293 One of the most surprising results in this study was the absence of ^{13}C-benzene cellular
294 incorporation in *Marinobacter* grown in coculture with *P. tricornutum,* despite strong ^{13}C-
295 benzene incorporation in *Marinobacter* grown in the absence of *P. tricornutum* (i.e., in PTspent
296 and ASW) and significant ^{12}C-benzene depletion in PT-*Marninobacter.* We repeated the
297 experiment and confirmed the results. These unexpected results suggest that in coculture with *P.*

298 *tricornutum, Marinobacter* obtained benzene, and possibly other hydrocarbons, directly from the
299 diatom rather than from the bulk medium. *Marinobacter* and *Roseibium* were sometimes
300 observed attached to *P. tricornutum.* Bacterial attachment or entry into the phycosphere [8] could
301 facilitate efficient VOC transfer directly from the diatom to the bacteria, before the chemicals
302 diffuse into the bulk medium. In coculture, direct VOC uptake from the diatom to *Marinobacter*
303 may occur via their physical interaction, enabling passive VOC diffusion across the diatom and
304 bacterial membranes. However, FadL outer membrane transporters can boost BTEX metabolism
305 in some Gram-negative hydrocarbon degraders [52], and the *Marinobacter* strain used in this study
306 encodes a FadL protein with 72% nucleotide identity to the well-characterized FadL in
307 *Escherichia coli*. In the presence of the diatom, *Marinobacter* may regulate FadL to optimize use
308 of a wide range of substrates delivered from *P. tricornutum*. However, FadL substrate specificity
309 and kinetics are not yet known, and FadL may become saturated, inhibiting BTEX uptake (i.e.,
310 added ^{13}C-benzene in our experiment) from the bulk medium. Bacteria also exhibit varying
311 preferences for BTEX substrates [53] and the benzenoid collection of hydrocarbons. Benzene may
312 be of lower value to *Marinobacter* compared to the full collection of VOC substrates from
313 growing *P. tricornutum,* or benzene may be oxidized to CO_2 in the coculture. Nevertheless, the
314 contrasting ^{13}C labeling results in *Marinobacter* suggest attachment dynamics in the *P.*
315 *tricornutum* phycosphere may have an important role in VOC uptake.

316 In the model set of phytoplankton and associated bacteria we investigated, phycosphere
317 resources were exploited by bacteria employing varying strategies: VOC specialists
318 (*Marinobacter* and *Roseibium*) that were motile and attached, generalists capable of VOC and
319 macromolecular uptake (*Rhodophyticola* and *Stappia*), and macromolecular specialists (*Yoonia*).
320 We propose that VOC specialists use chemotaxis to find and colonize the phycosphere, where

321 proximity to sources of low molecular weight, rapidly diffusing VOCs offers advantages [8].
322 Unknown is the duration of attachment or how hydrocarbon uptake is differentially regulated in
323 the presence and absence of *P. tricornutum*. The free-living generalists, *Rhodophyticola* and
324 *Stappia*, used VOCs and carbohydrate DOC and had fewer hydrocarbon oxidation genes.

325 Collectively, VOC use by phycosphere bacteria was surprisingly broad in the range of
326 compounds used and accounted for up to 29% of primary production by *P. tricornutum.* These
327 findings add support to previous reports of VOC uptake by bacteria and stimulation of
328 photosynthesis in phytoplankton co-cultured with VOC oxidizers. Previous reports show that
329 balanced production and consumption maintain low VOC concentrations in the oceans and have
330 associated VOC consumption with specialized metabolism in abundant, streamlined, non-motile
331 cells [54–57] but in the set of bacteria we studied some of the most active VOC utilizers were motile
332 and attached to the phytoplankton. Here, we show that the flux can be intercepted by VOC
333 specialists in the phycosphere, reducing ocean VOC accumulation and air-sea transfer. If the
334 proposed model for interpreting these results, that heterotroph consumption stimulates
335 photosynthesis because phytoplankton replenish lost VOC resources, is correct, then it is
336 conceivable that the mechanisms we described result in a global increase in ocean photosynthesis
337 and are an important conduit of direct transfer of GCP to bacteria that does not rely on the
338 influence of protistan grazing and virus predation.

339 Materials and methods:

340 *Culture growth and P. tricornutum physiology:*

341 *Phaeodactylum tricornutum* strain CCMP 2561 was maintained axenically and in
342 separate co-cultures with *Roseibium* sp. 13C1, *Yoonia* sp. 4BL, *Marinobacter* sp. 3-2,

343 *Rhodophyticola* sp. 6CLA, and *Stappia* sp. ARW1T. Cultures were grown under 12h:12h light:
344 dark cycles (60-70 µmole photons m^{-2} s^{-1}), at 19ºC in f/2+Si medium (ASW) [58]. DAPI (NucBlue,
345 Thermo Fischer) and fluorescence microscopy were used to check *P. tricornutum* axenicity.
346 Bacterial and diatom growth were determined in triplicate. Cell densities were measured using a
347 GUAVA flow cytometer (Millipore; Billerica, MA, USA) 1-2 h into the light phase. VOCs,
348 chlorophyll content (Chl*a*), and photosynthetic efficiency (F_v/F_m) were measured 4-6 h into the
349 light phase. Chl*a* was determined from filtering 2-5 ml of culture (GF/F, Whatman, 25 mm),
350 extracting in 5 ml 90% acetone, and storing at -20º C for 24 h. Chl*a* was quantified by
351 spectrophotometer (Shimadzu; Kyoto, Japan) [59]. F_v/F_m was measured by fast repetition-rate
352 fluorometer following 10 min dark acclimation [60]. Short-term carbon fixation rates
353 (approximating gross carbon production) were measured as in Moore et al. (2020). Axenic *P.*
354 *tricornutum* was grown in a closed system with culture headspace recirculating at 80 ml min^{-1} by
355 peristaltic pump and either directed back into the culture medium or passed first through a
356 hydrocarbon trap (Marineland Black Diamond Activated Carbon) and then into the medium. *P.*
357 *tricornutum*-bacteria cocultures were grown in the same manner with no hydrocarbon trap. All
358 flasks were recirculated for 24 h prior to inoculation with the cultures to remove background
359 VOCs. Samples for $^{14}CO_2$-uptake (10 ml) were collected by syringe during the *P. tricornutum*
360 exponential phase (2-4 x 10^5 cells ml^{-1}), spiked with 2 µCi of ^{14}C-sodium bicarbonate and
361 incubated 20 min in light or dark.
362
363 *VOC measurement by PTR-TOF/MS*

364 VOCs were quantitatively measured in axenic *P. tricornutum* and cocultures by PTR-TOF/MS
365 (Ionicon, Austria), as in Moore et al. (2020). Autoclaved ASW and HPLC-grade water were

366 measured alongside the samples as blank controls. Culture, ASW, or HPLC water (100 ml) was
367 transferred to a dynamic stripping chamber [56]and bubbled with breathing-grade air passed first
368 through a hydrocarbon trap and then through a glass frit in the bottom of the chamber at 50 ml
369 min^{-1} for 5 min to strip VOCs from the sample. PTR-TOF/MS data were analyzed using PTR
370 viewer 3.4.3 (Ionicon Analytik). Calibration and binning of m/z signals were performed as in
371 Moore et al. (2020). By using correlation plots and GLOVOCS [43], contaminants, fragments,
372 duplicates, and water clusters were removed; m/z signals were putatively identified using
373 GLOVOCS and Ionicon Viewer 3.4.1.

374 *Benzene uptake and nanoSIMS analyses*:

375 Benzene dose experiments were performed on *Rhodophyticola*, *Marinobacter*, and *Roseibium*.
376 *Stappia* could not be reliably grown in the absence of *P. tricornutum,* and *Yoonia* showed no
377 depletion of benzene in coculture. A saturated benzene solution was prepared in ASW and added
378 to *P. tricornutum*-spent media (prepared from 0.2 µm filtered spent media collected from axenic
379 *P. tricornutum* grown to 2-4 x 10^5 cells ml^{-1} and diluted in 1:10 with ASW) to achieve benzene
380 concentrations 0-180 µM with no headspace. Cultures were maintained at 19ºC in the dark.

381 ^{13}C-benzene uptake was evaluated using nanoSIMS in six different treatments grown in Teflon-
382 sealed borosilicate vials (*Marinobacter*) or airtight Nalgene bottles (*Rhodophyticola*). Fifty nM
383 98% ^{15}N leucine (Cambridge Isotopes, MA, USA) was added to all treatments as an independent
384 measure of cell activity (see Supp. table 9). Sample preparation for nanoSIMS and a brief
385 explanation of isotopic measurement are explained elsewhere (Supp. document 4). A CAMECA
386 NanoSIMS 50 was used to measure the isotopic composition of individual cells, explained in
387 detail elsewhere [61].

388 *SEM imaging*

389 Samples (5 ml) of *Marinobacter* and *Rhodophyticola* cocultured with *P. tricornutum* were
390 collected in mid-exponential phase, treated with 1.25 ml of 2X 5% glutaraldehyde + 2%
391 paraformaldehyde (PFA) in 0.1 M sodium cocadylate buffer (NaCB), incubated for 24 h, filtered
392 on a 0.2 µm polycarbonate filter, and washed three times with NaCB + Milli-Q water. The
393 filtered cells were subjected to critical point drying and then vacuum-dried and gold-coated.
394 Imaging was done using a detector with a 5.1 mm working distance, 1.8 kV voltage, and 20-30
395 µm aperture diameter at the Electron Microscope facility, LPSC, Oregon State University. The
396 number of bacteria adhered to *P. tricornutum* in coculture was estimated from 50 diatom cells.

397 *Genetic potential for hydrocarbon metabolism*

398 Whole genome sequences of each bacteria were acquired from NCBI (GB accession numbers:
399 *Marinobacter*: PRJNA500125; *Rhodophyticola*: PRJNA441682; Yoonia: PRJNA441685;
400 *Stappia*: PRJNA441689; *Roseibium*: PRJNA441686). Geneious Prime v2023.2.1 and Hidden
401 Markov Models were used to search genomes for proteins initiating hydrocarbon oxidation (i.e.,
402 *alkB*, Pfam(PF00487); *almA*, Pfam(PF00743); *rhdA*, Pfam(PF00848); *acmA*, Pfam(PF00743);
403 *aldH*, Pfam(PF00171) [62]. Each hit for *alkB* and *rhdA* was manually curated using Geneious
404 Prime v2023.2.1. Each hit was aligned using MUSCLE protein alignment in Geneious prime
405 v2023.2.1.

406 *Statistics*

407 Statistical analyses and figure construction were done in R studio v.4.1.1, with ggplot2 and
408 Complex heatmap packages [63,64]. Paired student t-tests were used to identify significant

differences between treatments. Benjamini-Hochberg corrections (Q-value cut-off ≤ 0.1) eliminated false positive m/z signals. Principle component analysis and Permutational Multivariate Analysis of Variance (PERMANOVA) were used to evaluate VOC accumulation and depletion patterns between cultures.

Acknowledgments

We thank Christina Ramon for lab assistance and Nicholas Baetge and Chih Ping Lee for assistance with data analysis. This research was supported by award ID OCE1948163 to K.H.H. and S.J.G. from the National Science Foundation, Biological Oceanography Program. Work at LLNL was Supported by the US Department of Energy's (DOE) Genomic Science Program through the LLNL μBioSpheres Science Focus Area grant # SCW1039 and performed under the auspices of the DOE under contract DE-AC52-07NA27344.

Author contributions

K.H.H., X.M., and V.G.P. conceived of the study. V.G.P. conducted all experiments with assistance from K.A., K.J., and L.C. and wrote the first manuscript draft with K.H.H. NanoSIMS analyses were conducted by X.M. and P.K.W. All authors contributed to final version of the manuscript.

References:

1. Fu, H., Uchimiya, M., Gore, J. & Moran, M. A. Ecological drivers of bacterial community assembly in synthetic phycospheres. *Proc Natl Acad Sci U S A* **117**, 3656–3662 (2020).

2. Seymour, J. R., Amin, S. A., Raina, J.-B. & Stocker, R. Zooming in on the phycosphere: the ecological interface for phytoplankton–bacteria relationships. *Nat Microbiol* **2**, 17065 (2017).

3. Mitchell, J. G., Okubo, A. & Fuhrman, J. A. Microzones surrounding phytoplankton form the basis for a stratified marine microbial ecosystem. *Nature 1985 316:6023* **316**, 58–59 (1985).

4. Seymour, J. R., Ahmed, T., Durham, W. M. & Stocker, R. Chemotactic response of marine bacteria to the extracellular products of Synechococcus and Prochlorococcus. *Aquatic Microbial Ecology* **59**, 161–168 (2010).

5. Smriga, S., Fernandez, V. I., Mitchell, J. G. & Stocker, R. Chemotaxis toward phytoplankton drives organic matter partitioning among marine bacteria. *Proc Natl Acad Sci U S A* **113**, 1576–1581 (2016).

6. Kogure, K., Simidu, U. & Taga, N. Bacterial attachment to phytoplankton in sea water. *J Exp Mar Biol Ecol* **56**, 197–204 (1981).

7. Ramanan, R. *et al.* Phycosphere bacterial diversity in green algae reveals an apparent similarity across habitats. *Algal Res* **8**, 140–144 (2015).

8. Raina, J. B. *et al.* Chemotaxis increases metabolic exchanges between marine picophytoplankton and heterotrophic bacteria. *Nature Microbiology 2023 8:3* **8**, 510–521 (2023).

9. Ugolini, G. S. *et al.* Microfluidic approaches in microbial ecology. *Lab Chip* **24**, 1394–1418 (2024).

10. Durham, B. P. *et al.* Cryptic carbon and sulfur cycling between surface ocean plankton. *Proc Natl Acad Sci U S A* **112**, 453–457 (2015).

11. Nouchi, I., Hosono, T. & Sasaki, K. Seasonal changes in fluxes of methane and volatile sulfur compounds from rice paddies and their concentrations in soil water. *Plant Soil* **195**, 233–245 (1997).

12. Brisson, V. *et al.* Identification of Effector Metabolites Using Exometabolite Profiling of Diverse Microalgae. *mSystems* **6**, (2021).

13. Russo, A., Pollastri, S., Ruocco, M., Monti, M. M. & Loreto, F. Volatile organic compounds in the interaction between plants and beneficial microorganisms. *J Plant Interact* **17**, 840–852 (2022).

14. Dawson, R. A. *et al.* The microbiology of isoprene cycling in aquatic ecosystems. *Aquatic Microbial Ecology* **87**, 79–98 (2021).

15. Shemi, A., Ben-Dor, S., Rotkopf, R., Dym, O. & Vardi, A. Phylogeny and biogeography of the algal DMS-releasing enzyme in the global ocean. *ISME Communications* **3**, (2023).

16. Asher, E., Dacey, J. W., Ianson, D., Peña, A. & Tortell, P. D. Concentrations and cycling of DMS, DMSP, and DMSO in coastal and offshore waters of the Subarctic Pacific during summer, 2010-2011. *J Geophys Res Oceans* **122**, 3269–3286 (2017).

466 17. Pozzer, A. C., Gómez, P. A. & Weiss, J. Volatile organic compounds in aquatic
467 ecosystems – Detection, origin, significance and applications. *Science of the Total*
468 *Environment* **838**, (2022).

469 18. Moore, E. R., Weaver, A. J., Davis, E. W., Giovannoni, S. J. & Halsey, K. H. Metabolism
470 of key atmospheric volatile organic compounds by the marine heterotrophic bacterium
471 Pelagibacter HTCC1062 (SAR11). *Environ Microbiol* **24**, 212–222 (2022).

472 19. Rocco, M. *et al.* Oceanic phytoplankton are a potentially important source of benzenoids
473 to the remote marine atmosphere. *Communications Earth & Environment 2021 2:1* **2**, 1–8
474 (2021).

475 20. Misztal, P. K. *et al.* Atmospheric benzenoid emissions from plants rival those from fossil
476 fuels. *Scientific Reports 2015 5:1* **5**, 1–10 (2015).

477 21. Moore, E. R., Davie-Martin, C. L., Giovannoni, S. J. & Halsey, K. H. Pelagibacter
478 metabolism of diatom-derived volatile organic compounds imposes an energetic tax on
479 photosynthetic carbon fixation. *Environ Microbiol* **22**, 1720–1733 (2020).

480 22. Wu, H. jun *et al.* Metagenomic analysis reveals specific BTEX degrading microorganisms
481 of a bacterial consortium. *AMB Express* **13**, (2023).

482 23. Bacosa, H. P., Mabuhay-Omar, J. A., Balisco, R. A. T., Omar, D. M. & Inoue, C.
483 Biodegradation of binary mixtures of octane with benzene, toluene, ethylbenzene or
484 xylene (BTEX): insights on the potential of Burkholderia, Pseudomonas and Cupriavidus
485 isolates. *World J Microbiol Biotechnol* **37**, 1–8 (2021).

486 24. Hocinat, A., Boudemagh, A., Ali-Khodja, H. & Medjemadj, M. Aerobic degradation of
487 BTEX compounds by Streptomyces species isolated from activated sludge and
488 agricultural soils. *Arch Microbiol* **202**, 2481–2492 (2020).

489 25. Khodaei, K., Nassery, H. R., Asadi, M. M., Mohammadzadeh, H. & Mahmoodlu, M. G.
490 BTEX biodegradation in contaminated groundwater using a novel strain (Pseudomonas
491 sp. BTEX-30). *Int Biodeterior Biodegradation* **116**, 234–242 (2017).

492 26. Jiang, B. *et al.* Biodegradation of Benzene, Toluene, Ethylbenzene, and o-, m-, and p-
493 Xylenes by the Newly Isolated Bacterium Comamonas sp. JB. *Appl Biochem Biotechnol*
494 **176**, 1700–1708 (2015).

495 27. Halsey, K. H. & Giovannoni, S. J. Biological controls on marine volatile organic
496 compound emissions: A balancing act at the sea-air interface. *Earth Sci Rev* **240**, 104360
497 (2023).

498 28. Rix, G. D. *et al.* Analysis of Essential Isoprene Metabolic Pathway Proteins in Variovorax
499 sp. Strain WS11. *Appl Environ Microbiol* **89**, (2023).

500 29. Halsey, K. H. *et al.* Biological cycling of volatile organic carbon by phytoplankton and
501 bacterioplankton. *Limnol Oceanogr* **62**, 2650–2661 (2017).

502 30. Yurimoto, H. & Sakai, Y. Interaction between C1-microorganisms and plants:
503 contribution to the global carbon cycle and microbial survival strategies in the
504 phyllosphere. *Biosci Biotechnol Biochem* **87**, 1–6 (2022).

505 31. Samo, T. J. *et al.* Attachment between heterotrophic bacteria and microalgae influences
506 symbiotic microscale interactions. *Environ Microbiol* **20**, 4385–4400 (2018).

507 32. Di Costanzo, F., Di Dato, V. & Romano, G. Diatom–Bacteria Interactions in the Marine
508 Environment: Complexity, Heterogeneity, and Potential for Biotechnological
509 Applications. *Microorganisms 2023, Vol. 11, Page 2967* **11**, 2967 (2023).

510 33. Wear, E. K., Carlson, C. A., Windecker, L. A. & Brzezinski, M. A. Roles of diatom
511 nutrient stress and species identity in determining the short- and long-term bioavailability
512 of diatom exudates to bacterioplankton. *Mar Chem* **177**, 335–348 (2015).

513 34. Liu, S. *et al.* Opportunities and challenges of using metagenomic data to bring uncultured
514 microbes into cultivation. *Microbiome* **10**, (2022).

515 35. Wang, Y., Zhao, Y., Bollas, A., Wang, Y. & Au, K. F. Nanopore sequencing technology,
516 bioinformatics and applications. *Nature Biotechnology 2021 39:11* **39**, 1348–1365 (2021).

517 36. Van Tol, H. M., Amin, S. A. & Virginia Armbrust, E. Ubiquitous marine bacterium
518 inhibits diatom cell division. *ISME J* **11**, 31–42 (2017).

519 37. Helliwell, K. E., Shibl, A. A. & Amin, S. A. The Diatom Microbiome: New Perspectives
520 for Diatom-Bacteria Symbioses. *The Molecular Life of Diatoms* 679–712 (2022)
521 doi:10.1007/978-3-030-92499-7_23/COVER.

522 38. Balakrishnan, R., de Silva, R. T., Hwa, T. & Cremer, J. Suboptimal resource allocation in
523 changing environments constrains response and growth in bacteria. *Mol Syst Biol* **17**,
524 10597 (2021).

525 39. Mayali, X. *et al.* Single-cell isotope tracing reveals functional guilds of bacteria associated
526 with the diatom Phaeodactylum tricornutum. *Nat Commun* **14**, 5642 (2023).

527 40. Kim, H. *et al.* Bacterial response to spatial gradients of algal-derived nutrients in a porous
528 microplate. *The ISME Journal 2021 16:4* **16**, 1036–1045 (2021).

529 41. Lang, X. P., He, Z., Yang, G. P. & Dai, G. Physiological responses and altered halocarbon
530 production in Phaeodactylum tricornutum after exposure to polystyrene microplastics.
531 *Ecotoxicol Environ Saf* **268**, 115702 (2023).

532 42. Cabrita, M. T., Vale, C. & Rauter, A. P. Halogenated Compounds from Marine Algae.
533 *Marine Drugs 2010, Vol. 8, Pages 2301-2317* **8**, 2301–2317 (2010).

534 43. Yáñez-Serrano, A. M. *et al.* GLOVOCS-Master compound assignment guide for proton
535 transfer reaction mass spectrometry users. *Atmos Environ* **244**, 117929 (2021).

536 44. Jakoncic, J., Jouanneau, Y., Meyer, C. & Stojanoff, V. The catalytic pocket of the ring-
537 hydroxylating dioxygenase from Sphingomonas CHY-1. (2006)
538 doi:10.1016/j.bbrc.2006.11.117.

539 45. Tan, H. M., Tang, H. Y., Joannou, C. L., Abdel-Wahab, N. H. & Mason, J. R. The
540 Pseudomonas putida ML2 plasmid-encoded genes for benzene dioxygenase are unusual in
541 codon usage and low in G + C content. *Gene* **130**, 33–39 (1993).

542 46. Bagnéris, C., Cammack, R. & Mason, J. R. Subtle Difference between Benzene and
543 Toluene Dioxygenases of Pseudomonas putida. *Appl Environ Microbiol* **71**, 1570 (2005).

544 47. Mangwani, N., Kumari, S. & Das, S. Involvement of quorum sensing genes in biofilm
545 development and degradation of polycyclic aromatic hydrocarbons by a marine bacterium
546 Pseudomonas aeruginosa N6P6. *Appl Microbiol Biotechnol* **99**, 10283–10297 (2015).

547 48. Olson, M. S., Ford, R. M., Smith, J. A. & Fernandez, E. J. Quantification of bacterial
548 chemotaxis in porous media using magnetic resonance imaging. *Environ Sci Technol* **38**,
549 3864–3870 (2004).

550 49. Lacal, J. *et al.* Bacterial chemotaxis towards aromatic hydrocarbons in Pseudomonas.
551 *Environ Microbiol* **13**, 1733–1744 (2011).

552 50. Matilla, M. A., Gavira, J. A. & Krell, T. Accessing nutrients as the primary benefit arising
553 from chemotaxis. *Curr Opin Microbiol* **75**, 102358 (2023).

554 51. Bell, W. & Mitchell, R. Chemotactic and growth responses of marine bacteria to algal
555 extracellular products. Biol. Bull. 143, 265–277 (1972).

556 52. Hearn, E. M., Patel, D. R. & Van Den Berg, B. Outer-membrane transport of aromatic
557 hydrocarbons as a first step in biodegradation. *Proc Natl Acad Sci U S A* **105**, 8601–8606
558 (2008).

559 53. Chicca, I. *et al.* Degradation of BTEX mixture by a new Pseudomonas putida strain: role
560 of the quorum sensing in the modulation of the upper BTEX oxidative pathway.
561 *Environmental Science and Pollution Research* **27**, 36203–36214 (2020).

562 54. Sun, J. *et al.* One Carbon Metabolism in SAR11 Pelagic Marine Bacteria. *PLoS One* **6**,
563 e23973 (2011).

564 55. Simó, R., Cortés-Greus, P., Rodríguez-Ros, P. & Masdeu-Navarro, M. Substantial loss of
565 isoprene in the surface ocean due to chemical and biological consumption.
566 *Communications Earth & Environment 2022 3:1* **3**, 1–8 (2022).

567 56. Davie-Martin, C. L., Giovannoni, S. J., Behrenfeld, M. J., Penta, W. B. & Halsey, K. H.
568 Seasonal and Spatial Variability in the Biogenic Production and Consumption of Volatile
569 Organic Compounds (VOCs) by Marine Plankton in the North Atlantic Ocean. *Front Mar*
570 *Sci* **7**, (2020).

57. Halsey, K. H. *et al.* Biological cycling of volatile organic carbon by phytoplankton and bacterioplankton. *Limnol Oceanogr* **62**, 2650–2661 (2017).

58. Guillard, R. R. L. & Ryther, J. H. STUDIES OF MARINE PLANKTONIC DIATOMS: I. CYCLOTELLA NANA HUSTEDT, AND DETONULA CONFERVACEA (CLEVE) GRAN. *Can J Microbiol* **8**, 229–239 (1962).

59. Ritchie, R. J. Consistent Sets of Spectrophotometric Chlorophyll Equations for Acetone, Methanol and Ethanol Solvents. *Photosynth Res* **89**, 27–41 (2006).

60. Kolber, Z. S., Prášil, O. & Falkowski, P. G. Measurements of variable chlorophyll fluorescence using fast repetition rate techniques: defining methodology and experimental protocols. *Biochimica et Biophysica Acta (BBA) - Bioenergetics* **1367**, 88–106 (1998).

61. Dekas, A. E. *et al.* Characterizing Chemoautotrophy and Heterotrophy in Marine Archaea and Bacteria With Single-Cell Multi-isotope NanoSIP. *Front Microbiol* **10**, 455124 (2019).

62. Apweiler, R. *et al.* The Universal Protein Resource (UniProt) 2009. *Nucleic Acids Res.* **37**, D169–D174 (2008).

63. Gu, Z. Complex heatmap visualization. *iMeta* **1**, (2022).

64. Gu, Z., Eils, R. & Schlesner, M. Complex heatmaps reveal patterns and correlations in multidimensional genomic data. *Bioinformatics* **32**, 2847–2849 (2016).

Figures and tables:

Table 1: Traits of bacteria used in this study

Bacteria	Carbohydrate metabolism[a]	Hydrocarbon metabolism[b]	Motility	Chemotaxis (*che* genes)	Attachment to diatom[c]
Marinobacter	+	+++	Yes	Yes	Yes
Roseibium	+	+++	Yes	Yes	Yes
Rhodophyticola	+++	++	No	No	No
Stappia	+++	++	No	No	No
Yoonia	+++	+	No (?)	Yes	Yes

[a]Summarized from Mayali et al. 2023
[b]Summarized from Fig. 2.
[c]Mayali et al. 2023 and this study

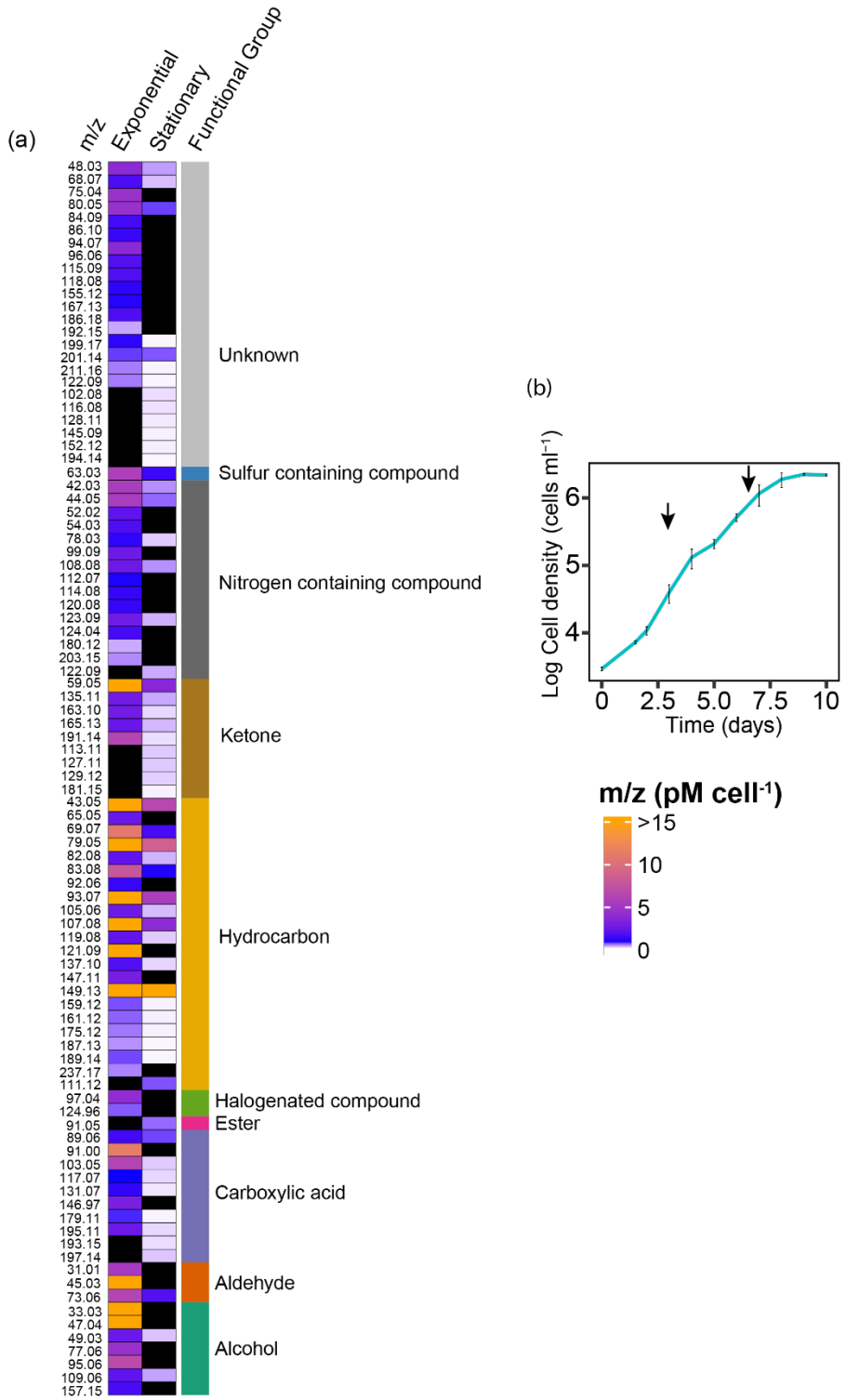

Figure 1: VOC production in P. tricornutum. a. Cell-normalized concentrations of m/z values (rows) ranging from low (light blue) to high (orange) concentrations produced during exponential and stationary phases. Black are m/z values that were not significantly higher than the media control. Functional group classifications for each m/z+1 value are shown in the rightmost column. b. P. tricornutum growth (n=6 independent cultures). Arrows indicate sampling days for VOCs.

597

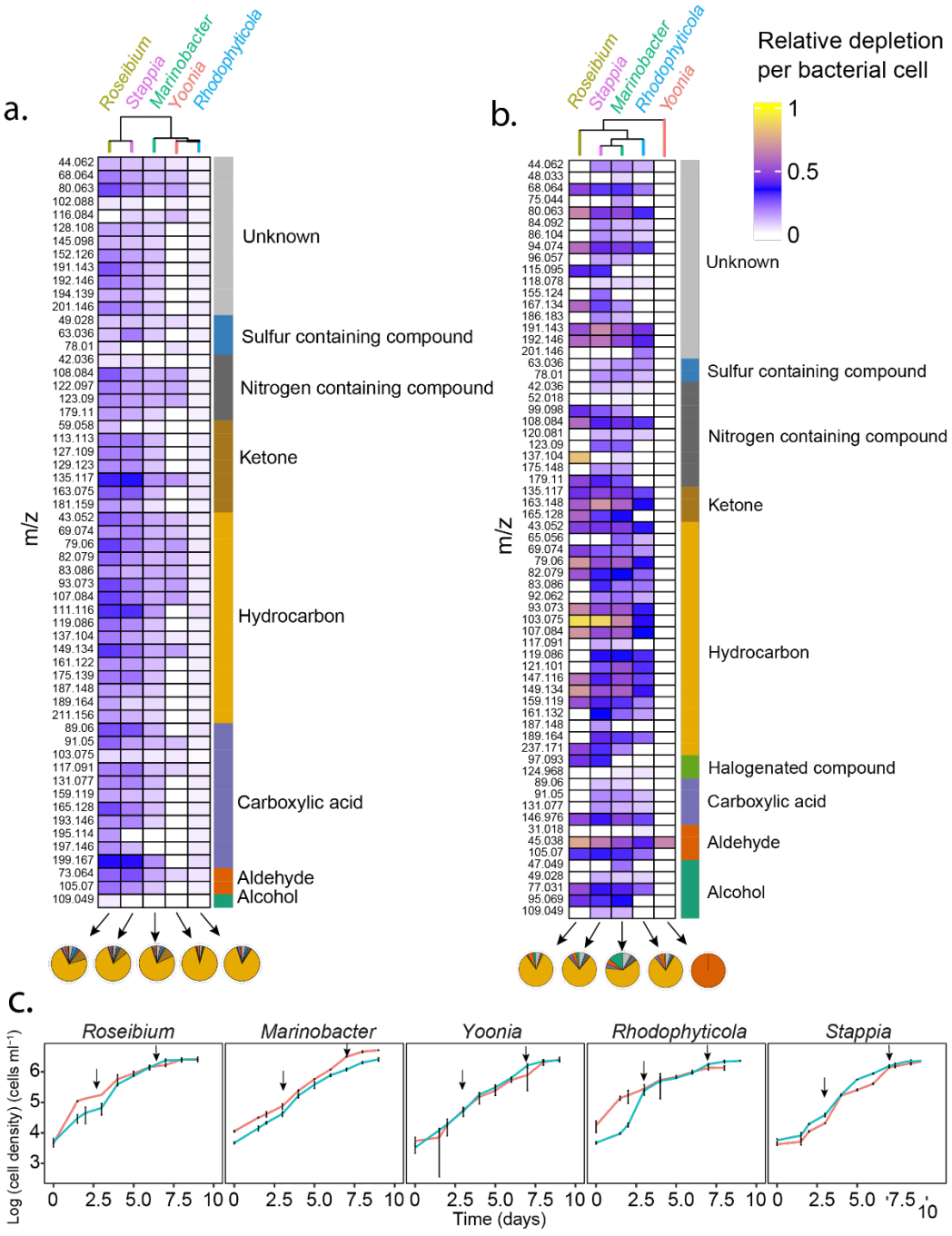

d.

Bacterial species	*alkB*	*rhdA*	*bnzA*	*bnzB*	*almA*	*aor*	*acmA*
Marinobacter	2	1	1	1	2	1	2
Yoonia	0	0	0	0	0	2	0
Rhodophyticola	2	0	1	0	0	1	0
Roseibium	2	1	1	0	2	2	1
Stappia	0	0	0	0	1	1	1

Figure 2: Phycosphere bacteria demonstrate widely ranging VOC depletion patterns. a. m/z+1 depletion (rows) in each P. tricornutum–bacteria coculture (columns are labeled with the bacteria grown with P. tricornutum) in exponential (a) and stationary phase (b) relative to axenic P. tricornutum in each of the growth phases. The magnitude of depletion is shown ranging from low (light blue) to high (yellow). Pearson correlation distances were used to cluster depletion patterns between PT-bacteria cocultures (top axes). Pie charts show the proportion of the total depleted VOC concentration in each functional group.(c) Growth of each bacteria (red lines) in coculture with P. tricornutum (blue lines), (n=6). Arrows indicate sampling day for VOCs. d. Genetic potential for hydrocarbon metabolism in the phycosphere bacteria. Number of gene copies is shown for each bacteria. Abbreviations: alkB (alkane-1-monooxygenase), bnzA (benzene dioxygenase alpha-subunit), bnzB (benzene dioxygenase beta-subunit), almA (flavin-binding monooxygenase), aor (aldehyde oxidoreductase), acmA (acetone monooxygenase).

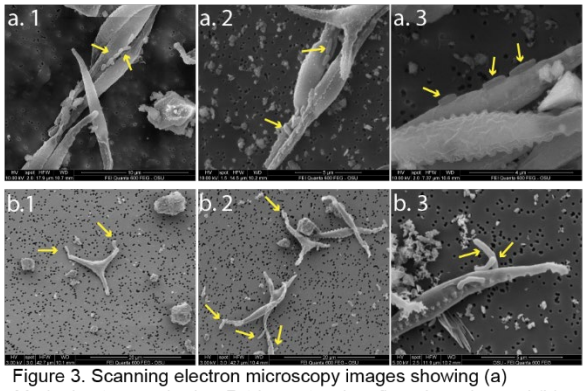

Figure 3. Scanning electron microscopy images showing (a) *Marinobacter* attached to *P. tricronutum* in a flat orientation and (b) *Roseibium* attached to *P. tricornutum* in polar orientation.

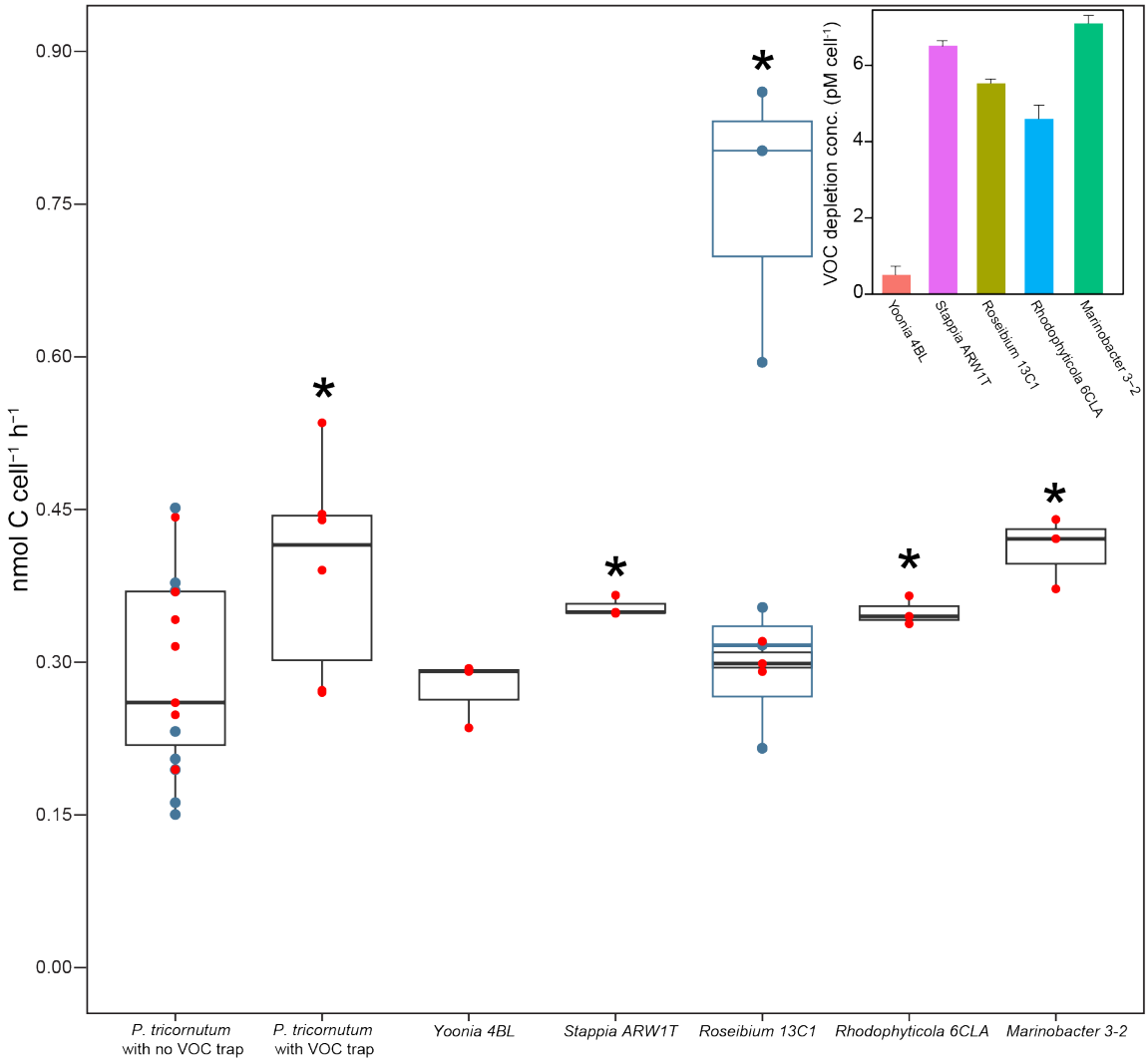

Figure 4: Photosynthetic carbon fixation in P. tricornutum in the presence and absence of VOC sinks (hydrocarbon trap or each bacteria in coculture). Points are short term (10 min) carbon fixation rates for each culture or coculture. Box plots show the mean and upper and lower quartile divisions; whiskers show 95% confidence limits. *p-value < 0.01; t-test. Inset shows the total bacterial cell-normalized VOC depletion in each P. tricornutum-bacteria coculture.

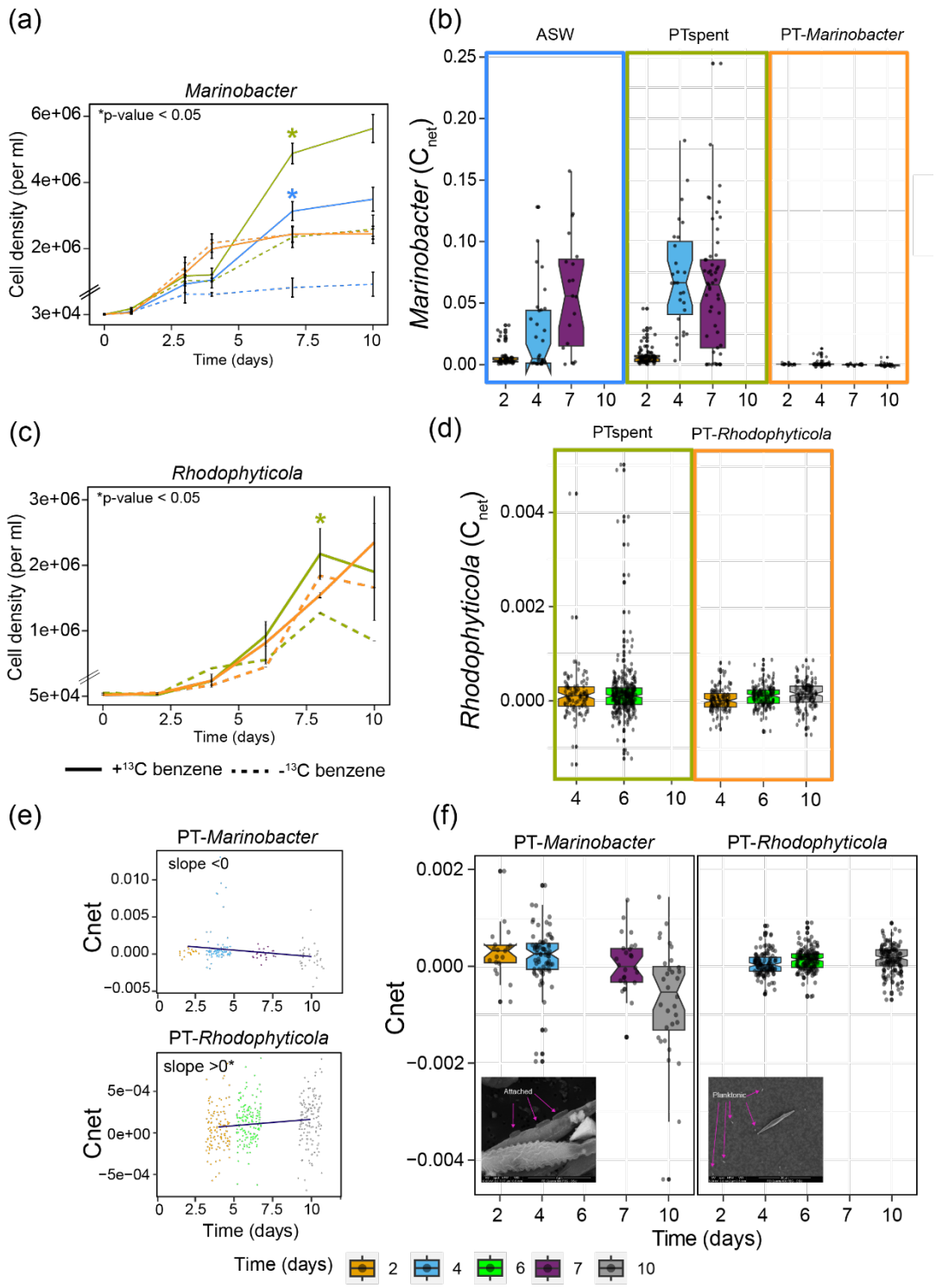

Figure 5: Benzene incorporation into Marinobacter and Rhodophyticola biomass (a,c) Bacterial cell densities in the presence (solid lines) and absence (dashed lines) of 13C benzene in ASW (blue), Ptspent (olive), and coculture with P. tricornutum (orange). Asterisks indicate treatments with significant increases in cell densities in the presence of benzene. (b, d) 13C enrichment in Marinobacter and Rhodophyticola in ASW (Marinobacter only), Ptspent, and in coculture with P. tricornutum. Cnet is the fraction of biomass labelled from 13C benzene. (e) Linear regression of bacterial 13C benzene enrichment in PT-Marinobacter (top) and PT-Rhodophyticola (bottom). Student t-test *p-value < 0.05. (f) Expanded y-axis showing bacterial Cnet values in cocultures and inset SEM images of Marinobacter attached to P. tricornutum and Rhodophyticola unattached.

601

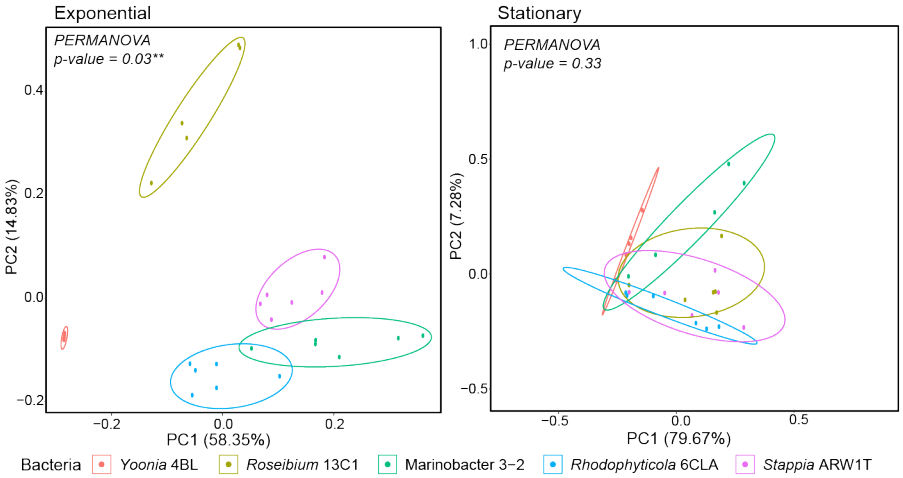

Supp. fig. 1: Principal coordinate analysis of depleted VOCs in *P. tricornutum*–bacteria cocultures in exponential (left) and stationary (right) growth phases.

602

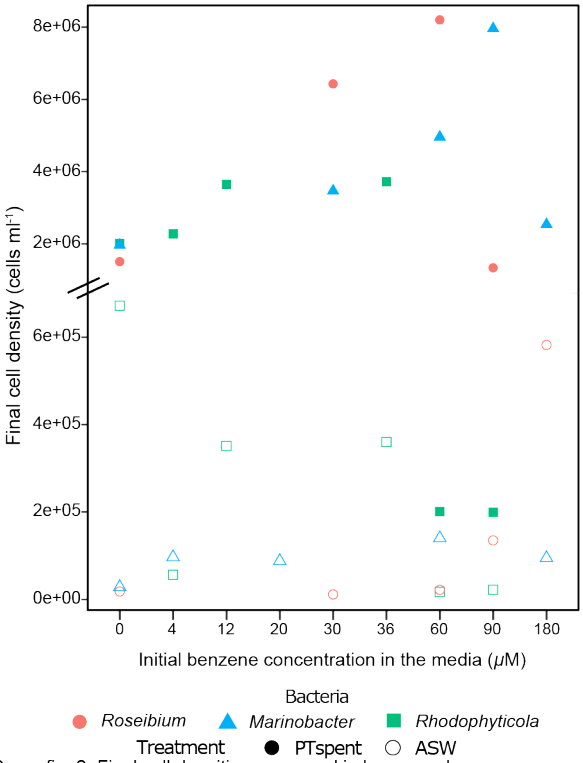

Supp. fig. 2: Final cell densities measured in benzene dose experiments. Each bacterium was inoculated into Ptspent (filled symbols) and ASW media (open symbols) with initial benzene concentrations 0-180 μM. *Roseibium* (circles), *Marinobacter* (triangles), and *Rhodophyticola* (squares).

603

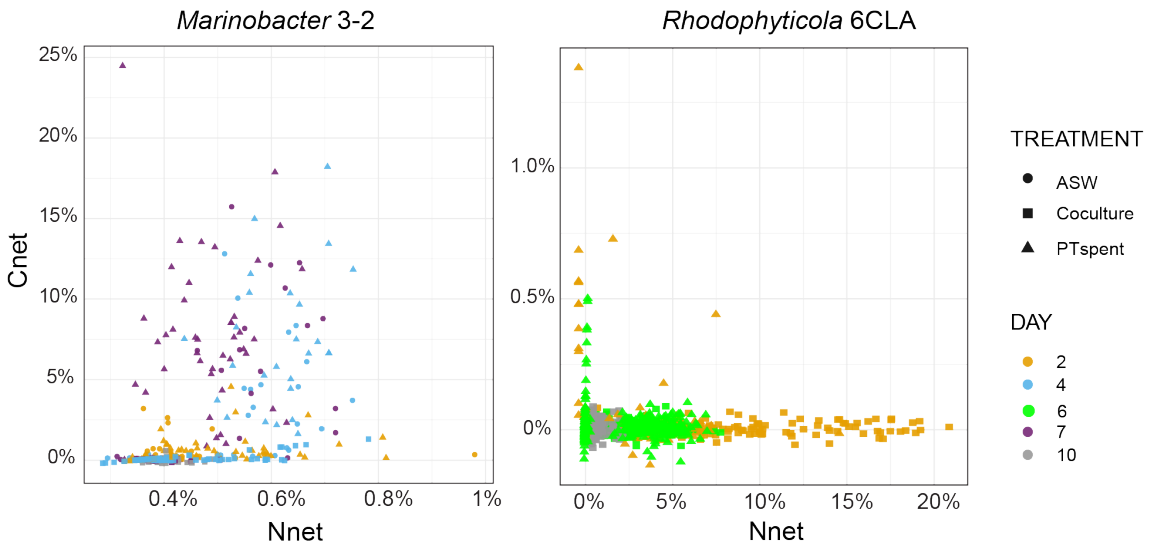

Supp. fig. 3: Cnet vs Nnet in *Marinobacter* and *Rhodophyticola* measured in three different treatments.